
This is an electronic reprint of the original article.
This reprint may differ from the original in pagination and typographic detail.

Huang, Yike; Nguyen, Kha; Natarajan, Ashwin; Kuzyk, Anton
A DNA Origami-Based Chiral Plasmonic Sensing Device

Published in:
ACS Applied Materials and Interfaces

DOI:
[10.1021/acsami.8b19153](https://doi.org/10.1021/acsami.8b19153)

Published: 26/12/2018

Document Version
Publisher's PDF, also known as Version of record

Published under the following license:
Other

Please cite the original version:
Huang, Y., Nguyen, K., Natarajan, A., & Kuzyk, A. (2018). A DNA Origami-Based Chiral Plasmonic Sensing Device. *ACS Applied Materials and Interfaces*, 10(51), 44221-44225. <https://doi.org/10.1021/acsami.8b19153>

This material is protected by copyright and other intellectual property rights, and duplication or sale of all or part of any of the repository collections is not permitted, except that material may be duplicated by you for your research use or educational purposes in electronic or print form. You must obtain permission for any other use. Electronic or print copies may not be offered, whether for sale or otherwise to anyone who is not an authorised user.

A DNA Origami-Based Chiral Plasmonic Sensing Device

Yike Huang,^{*,†} Minh-Kha Nguyen,^{†,‡} Ashwin Karthick Natarajan,[†] Vu Hoang Nguyen,[†] and Anton Kuzyk^{*,†}

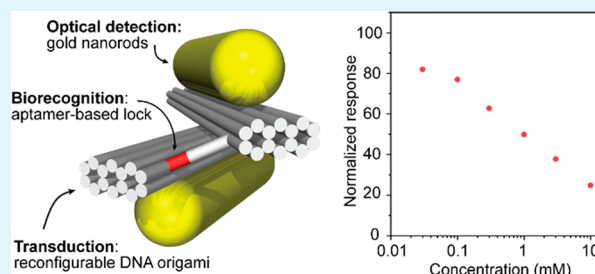
[†]Department of Neuroscience and Biomedical Engineering, Aalto University School of Science, Aalto FI-00076, Finland

[‡]Faculty of Chemical Engineering, HCMC University of Technology, VNU-HCM, Ho Chi Minh City 70000, Vietnam

Supporting Information

ABSTRACT: Accurate and reliable biosensing is crucial for environmental monitoring, food safety, and diagnostics. Spatially reconfigurable DNA origami nanostructures are excellent candidates for the generation of custom sensing probes. Here we present a nanoscale biosensing device that combines the accuracy and precision of the DNA origami nanofabrication technique, unique optical responses of chiral plasmonic assemblies, and high affinity and selectivity of aptamers. This combination enables selective and sensitive detection of targets even in strongly absorbing fluids. We expect that the presented sensing scheme can be adapted to a wide range of analytes and tailored to specific needs.

KEYWORDS: DNA origami, gold nanorods, chiral plasmonics, aptamers, biosensing



Various materials and biochemical entities have properties that are potentially useful for biorecognition and/or transduction in sensing applications.¹ The difficulty often lies in the integration of those properties for the realization of efficient and reliable biosensors. This is especially challenging for nanoscale sensing devices. Herein, we describe design, fabrication, and characterization of a nanoscale sensing device that combines the beneficial biosensing properties of DNA origami technique, chiral plasmonics, and aptamers.

DNA nanotechnology, which utilizes DNA as a construction material for the assembly of nanostructures,^{2,3} is finding increasing use in biosensing applications.⁴ Recently, the DNA origami technique has emerged as a powerful method for fabrication of complex nanostructures that can serve as templates for assembly of various functional components with nanometer precision.^{5–10} In addition, reconfigurable DNA origami structures have enabled realization of nanoscale devices with functionalities tailored for the characterization of bimolecular interactions,^{11–13} biosensing,^{14–17} and drug delivery.¹⁸

Metal nanostructures and their plasmon resonances have been extensively used as optical transducers for sensing. Utility of plasmonics traditionally has stemmed from the ability to generate strong electromagnetic field enhancement.¹⁹ Alternatively, the coupling of plasmonic excitations in metal nanoparticles and its sensitivity to interparticle distances can be utilized for sensing.^{20,21} Among coupled plasmonic systems, reconfigurable chiral plasmonic assemblies enabled by DNA nanotechnology²² are particularly promising candidates for sensing applications because their structural configurations can be readily correlated with the optical responses, e.g., circular dichroism (CD).²³ Optical detection based on CD spectroscopy

provides several additional benefits: biological samples exhibit very low background CD signals in the visible spectrum and optical measurements can be performed even in strongly absorbing fluids.²⁴ Recently, a DNA origami-based chiral plasmonic nanosensor with ability to detect viral RNA at concentrations down to 100 pM has been demonstrated.¹⁷ The sensitivity to RNA has been implemented using DNA-based molecular “lock” as a biorecognition element. In order to extend the applicability of DNA origami-based plasmonic nanosensors beyond nucleic acids, more universal biorecognition elements are required. Nucleic acids aptamers are excellent candidates. Aptamers with high affinity and specificity have been selected against a wide variety of target molecules including small molecules, peptides, and proteins.²⁵ Furthermore, aptamers are easy to generate, have low production cost and batch-to-batch variability, and can be easily incorporated into DNA origami structures.

The design of our DNA origami-based chiral nanosensor is schematically illustrated in Figure 1A. A DNA aptamer-based molecular lock is employed as a biorecognition element. The lock is incorporated into reconfigurable DNA origami-AuNRs construct and defines the spatial configuration state of the nanosensor. The DNA origami structure consists of two 14-helix bundles (80 nm × 16 nm × 8 nm) linked in the center by two flexible single-stranded segments. Depending on the relative orientation of the two bundles, the structure can adapt left- or right-handed (LH/RH) chiral spatial configuration with ~50° angle between the bundles.²⁶ Two gold

Received: November 1, 2018

Accepted: December 7, 2018

Published: December 7, 2018

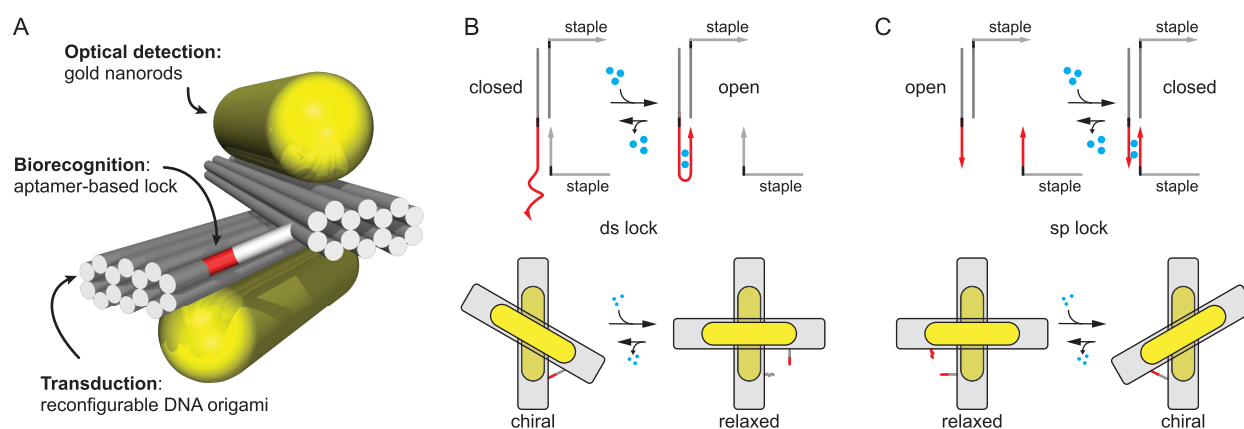


Figure 1. Design and operation principle. (A) Schematics of the DNA origami-based chiral plasmonic nanosensor. The DNA aptamer-based molecular lock is employed as a biorecognition element incorporated into reconfigurable DNA origami structure, which hosts two gold nanorods (AuNRs). Two AuNRs constitute a three-dimensional (3D) chiral plasmonic object with circular dichroism optical response that is dependent on the angle between the rods. (B,C) Operation principle of the nanosensor with different aptamer-based molecular locks. (B) Double-stranded (ds)-lock opens upon target binding, and the 3D spatial configuration of the origami-AuNR construct changes from chiral to relaxed. (C) Split aptamer (sp)-lock closes upon target binding, and the spatial configuration of origami-AuNR constructs changes from relaxed to chiral.

nanorods (AuNRs), 55 nm \times 23 nm, are assembled on top of the DNA origami to enable optical detection of the chiral configuration with CD spectroscopy.^{17,26–28} Detailed description of the DNA origami design and AuNRs assembly is provided in the [Supporting Information](#).

The operation principle of the nanosensor is illustrated in [Figure 1B, C](#). The state of the aptamer-based lock changes upon target binding. The DNA origami structure transduces the state of the lock (closed/open) into two spatial configurations of the AuNRs dimer (chiral/relaxed) with distinct plasmonic CD responses.^{26–28} To demonstrate the versatility of our system, we designed two types of locks. The double stranded (ds)-lock consisted of an aptamer and a complementary strand (cs) and undergoes closed to open transition upon analyte binding ([Figure 1B](#)). The split aptamer (sp)-lock consisted of partial aptamer strands and closes upon target binding ([Figure 1C](#)). In both cases, we used adenosine as a model analyte and adapted its corresponding DNA aptamer.^{29,30}

Agarose gel electrophoresis, transmission electron microscopy (TEM), and CD spectroscopy were used to characterize the assembly of the DNA origami-AuNRs structures. The structures assembled with high yields ([Figure 2A](#) and [Figure S1 and S2](#)) and exhibited distinct CD responses in chiral and relaxed states ([Figure 2B](#)). The relaxed state had a slight RH CD response preference due to structural imperfections.

First, we tested the performance of nanosensors with ds-locks ([Figure 1B](#)). The polyacrylamide gel electrophoresis ([Figure S4](#)) showed the shortest length of cs to form a stable hybrid with the aptamer is 12 nt (cs12) and that this hybridization was efficiently broken by adenosine as the adenosine competed against the cs to bind with the aptamer ([Figure S5](#)). The sequences of the aptamer and the cs12 were incorporated into the two origami bundles as ds12-lock ([Figure S6A](#)) and the origami was in RH chiral state when the ds12-lock was closed. The agarose gel electrophoresis showed that the origami with the ds12-lock shifted faster compared to the relaxed structure confirming the closed configuration ([Figure S7](#)). After the attachment of AuNRs, the DNA origami-AuNRs constructs with the ds12-lock (ds12-nanosensor) exhibited strong RH CD response. Addition of

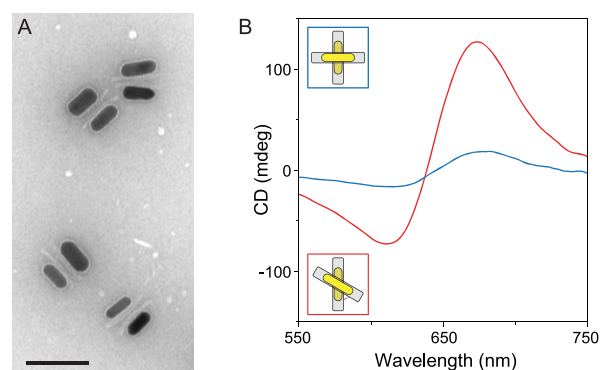


Figure 2. DNA origami-AuNR structures and their chiroptical responses. (A) TEM image of the DNA origami-AuNR structures. The structures showed typical binding preference to the TEM grid, i.e., parallel origami bundles and rods. Scale bar, 100 nm. (B) CD responses in RH chiral (red line) and relaxed (blue line) states.

adenosine resulted in a concentration dependent decrease of the CD signal, indicating the equilibrium shift from the RH chiral state to the relaxed state ([Figure 3A](#)). The lowest concentration of adenosine to induce clear change in CD spectra was 300 μ M. The highest measured adenosine

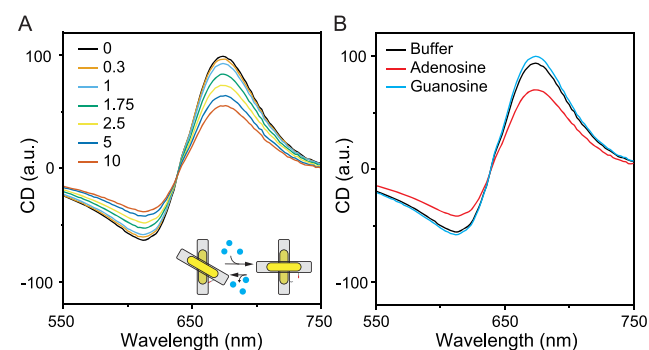


Figure 3. Ds12-nanosensor. (A) Relative CD responses at different concentrations of adenosine. Concentrations are given in mM. (B) CD responses of the nanosensor in the presence of adenosine (2 mM) or guanosine (saturated solution, 2.5 mM).

concentration was 10 mM due to the limited solubility. The typical response time of the ds12-nanosensor was in the range of tens of minutes (Figure S11) and the limit of detection (LOD) was $\sim 270 \mu\text{M}$ (see the Supporting Information). To demonstrate that the CD change was induced by the specific interaction between the aptamer-based lock and the adenosine, we constructed the structures in which the aptamer strand in the lock was replaced by a scramble strand that formed the same 12 base pairs (bp) with the cs12 sequence but lacked the ability to bind adenosine. No adenosine response was observed when the aptamer sequence was scrambled or omitted (Figure S8). The ds12-nanosensor also responded to the adenosine triphosphate (ATP), which is another target of the adenosine aptamer (Figure S9). No decrease in the CD signal was observed in the presence of the guanosine (Figure 3B), which confirms the selectivity of our sensing device.

To test whether the ds-lock can be used to detect adenosine at concentrations below $300 \mu\text{M}$, we shortened the hybridization length between the aptamer and the cs from 12 bp to 9 bp by substituting the cs12 with the cs9 sequence (ds9-lock, Table S2). Fewer base pairs of the aptamer-cs hybrid are expected to benefit the competing binding between the adenosine and the aptamer. Although free cs9 and aptamer were not expected to form a stable hybrid at room temperature the origami-AuNRs constructs with the ds9-lock (ds9-nanosensor) exhibited strong CD signals, possibly due to the enhanced local concentration effect after the incorporation into the origami structures. The ds9-nanosensor exhibited clear CD changes at the adenosine concentration of $30 \mu\text{M}$ (Figure 4A), 1 order of magnitude smaller than the ds12-nanosensor. The LOD of ds9-nanosensor was $\sim 20 \mu\text{M}$. Furthermore, the ds9-nanosensor responded to the addition of adenosine within 1 min (Figure S11), much faster than ds12-nanosensor. Although shortening the hybridization length of the ds-lock

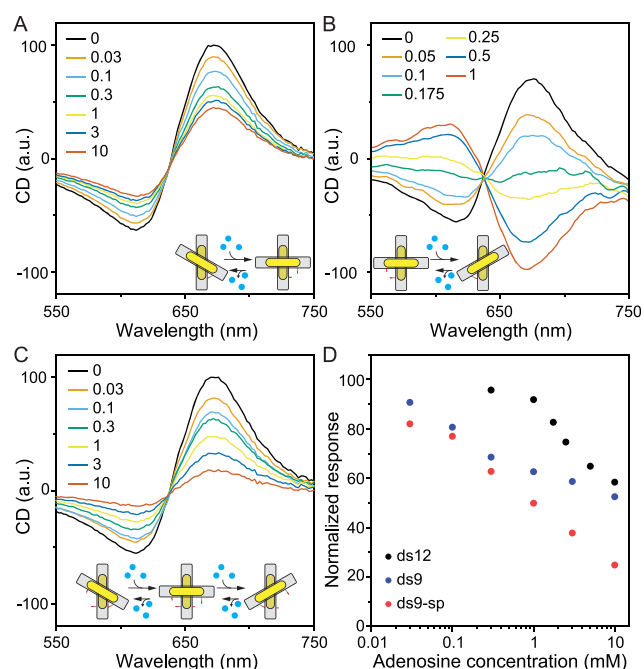


Figure 4. Relative CD responses of the (A) ds9-nanosensor, (B) sp-nanosensor, and (C) ds9-sp-nanosensor at different adenosine concentrations. Concentrations are given in mM. (D) Relative CD signals at 612 nm at different concentrations of adenosine.

improved the detection limit and speed, the correlation between the CD signal and the adenosine concentration became less steep (Figure 4D).

Next, we tested the performance of the nanosensor with the split aptamer (sp)-molecular lock (Figure 1C), which consisted of two partial aptamers (apt1, apt2) that do not interact with each other but can form an apt1-apt2-adenosine complex in the presence of the adenosine. We inserted the apt1 and apt2 on the two bundles of the origami as shown in the Figure S6B. The complex formation of apt1-apt2-adenosine enabled the origami to possess a LH chiral configuration. The CD spectra of the origami-AuNRs with the sp-lock (sp-nanosensor) in adenosine showed that the higher the adenosine concentration, the higher the LH CD signal generated (Figure 4B). Of note, although the LH CD spectra became clear only after the adenosine concentration reached $250 \mu\text{M}$, the RH CD signal of the relaxed state exhibited clear decrease in CD at $50 \mu\text{M}$ of adenosine. The high adenosine concentration was required to compensate the constructs' intrinsic tendency toward the RH configuration in the relaxed state. The LOD of sp-nanosensor was $\sim 65 \mu\text{M}$. When the sp-lock was inserted on the opposite side of the origami bundle to close the construct as the RH structure, the signal started to increase at $25 \mu\text{M}$ (Figure S10).

The DNA origami technique provides the ability to combine both types of locks in one device. We used the ds9-lock responsible for RH chiral to relaxed transition and sp-lock responsible for relaxed to LH chiral transition to test the performance of the dual lock system (ds9-sp-nanosensor). The addition of adenosine is expected to open the ds9-lock to drive the equilibrium from the RH toward the relaxed state and close the sp-lock to shift the equilibrium from the relaxed to the LH state. The ds9-sp-nanosensor not only showed clear change in CD already at $30 \mu\text{M}$ of adenosine (Figure 4C), similar to ds9-lock based system, but also exhibited steeper CD signal-adenosine concentration dependence (Figure 4D) compared to the nanosensor with only ds9-lock. The LOD of ds9-sp-nanosensor was $\sim 25 \mu\text{M}$. In addition, the response time of the double lock-nanosensor was in the range of several minutes (Figure S11).

Finally, we tested our devices in absorbing fluids. The CD responses of the nanosensor were almost identical at optical densities of environment up to $\text{OD} \approx 3$ (Figure 5). At ODs above 3, the CD response became too noisy for reliable measurement.

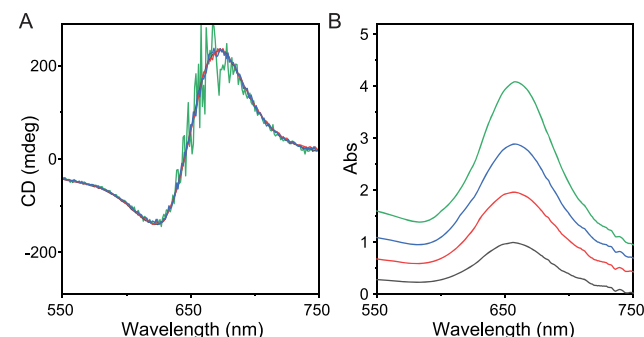


Figure 5. CD responses of the nanosensor in absorbing fluids. (A) CD spectra of the ds9-sp-nanosensor in environments with different optical extinction. (B) Corresponding absorption spectra. The absorption was adjusted by addition of gold nanorods.

In summary, we developed a nanoscale biosensing device that combines the benefits of the DNA origami technique, chiral plasmonics and aptamers. One of the main advantages of such combination is the high level of programmability. Aptamer based biorecognition elements can be easily incorporated into DNA origami structures at desired locations. While the availability of split aptamers is limited, the double stranded lock strategy can be adapted to a wide variety of aptamers and targets. Dynamic DNA origami structures can be optimized to undergo desired spatial reconfiguration upon target binding and the spectral position of optical responses can be tuned by the size and material composition of the nanorods. In addition, the nanosensor enables optical detection in environments with strong optical extinction, which would simplify preparation procedures of biologically relevant samples. Our results demonstrate a promising route toward the development of the aptamer-based sensing platforms utilizing optical responses of chiral plasmonic nanostructures.

■ ASSOCIATED CONTENT

■ Supporting Information

The Supporting Information is available free of charge on the ACS Publications website at DOI: 10.1021/acsami.8b19153.

Materials, experimental details, gel electrophoresis images, TEM images, and absorption and CD spectra (PDF)

■ AUTHOR INFORMATION

Corresponding Authors

*E-mail: yike.huang@aalto.fi.

*E-mail: anton.kuzyk@aalto.fi.

ORCID

Yike Huang: 0000-0003-2559-432X

Minh-Kha Nguyen: 0000-0003-3456-3162

Ashwin Karthick Natarajan: 0000-0001-7897-708X

Anton Kuzyk: 0000-0001-8060-6122

Author Contributions

A.K. and Y.H. conceived the research and designed the experiments. K.N. synthesized the AuNRs. Y.H. prepared the samples with the help of V.N., conducted the gel electrophoresis experiments, and performed the CD measurements. A.K. and A.N. performed TEM characterization. A.K. and Y.H. wrote the manuscript with the contributions of all authors. All authors have given approval to the final version of the manuscript.

Funding

This work was supported by the Academy of Finland (grant 308992 (A.K., A.K.N.)) and the European Union's Horizon 2020 research and innovation program under the Marie Skłodowska-Curie grant agreement 71364 (Y.H.).

Notes

The authors declare no competing financial interest.

■ ACKNOWLEDGMENTS

We thank S. Voutilainen for assistance with the CD spectrometer, T. Liedl for the useful discussions, and I. Smalyukh for the gift of nanorods used for the initial experiments. We acknowledge the provision of facilities and technical support by Aalto University at OtaNano-Nano-microscopy Center (Aalto-NMC).

■ REFERENCES

- (1) Touhami, A. Biosensors and Nanobiosensors: Design and Applications. In *Nanomedicine*; Seifalian, A., de Mel, A., Kalaskar, D. M., Eds.; One Central Press, 2014; Chapter 15, pp 374–403.
- (2) Seaman, N. C.; Sleiman, H. F. DNA Nanotechnology. *Nat. Rev. Mater.* **2017**, *3*, 17068.
- (3) Krishnan, Y.; Simmel, F. C. Nucleic Acid Based Molecular Devices. *Angew. Chem., Int. Ed.* **2011**, *50*, 3124–3156.
- (4) Lu, C.-H.; Willner, B.; Willner, I. DNA Nanotechnology: From Sensing and DNA Machines to Drug-Delivery Systems. *ACS Nano* **2013**, *7*, 8320–8332.
- (5) Rothmund, P. W. K. Folding DNA to Create Nanoscale Shapes and Patterns. *Nature* **2006**, *440*, 297–302.
- (6) Wang, P.; Meyer, T. A.; Pan, V.; Dutta, P. K.; Ke, Y. The Beauty and Utility of DNA Origami. *Chem.* **2017**, *2*, 359–382.
- (7) Hong, F.; Zhang, F.; Liu, Y.; Yan, H. DNA Origami: Scaffolds for Creating Higher Order Structures. *Chem. Rev.* **2017**, *117*, 12584–12640.
- (8) Kuzyk, A.; Jungmann, R.; Acuna, G. P.; Liu, N. DNA Origami Route for Nanophotonics. *ACS Photonics* **2018**, *5*, 1151–1163.
- (9) Liu, N.; Liedl, T. DNA-Assembled Advanced Plasmonic Architectures. *Chem. Rev.* **2018**, *118*, 3032–3053.
- (10) Ke, Y.; Castro, C.; Choi, J. H. Structural DNA Nanotechnology: Artificial Nanostructures for Biomedical Research. *Annu. Rev. Biomed. Eng.* **2018**, *20*, 375–401.
- (11) Funke, J. J.; Ketterer, P.; Lieleg, C.; Schunter, S.; Korber, P.; Dietz, H. Uncovering the Forces between Nucleosomes Using DNA Origami. *Sci. Adv.* **2016**, *2*, e1600974.
- (12) Le, J. V.; Luo, Y.; Darcy, M. A.; Lucas, C. R.; Goodwin, M. F.; Poirier, M. G.; Castro, C. E. Probing Nucleosome Stability with a DNA Origami Nanocaliper. *ACS Nano* **2016**, *10*, 7073–7084.
- (13) Nickels, P. C.; Wunsch, B.; Holzmeister, P.; Bae, W.; Kneer, L. M.; Grohmann, D.; Tinnefeld, P.; Liedl, T. Molecular Force Spectroscopy with a DNA Origami-Based Nanoscopic Force Clamp. *Science* **2016**, *354*, 305–307.
- (14) Kuzuya, A.; Sakai, Y.; Yamazaki, T.; Xu, Y.; Komiyama, M. Nanomechanical DNA Origami “Single-Molecule Beacons” Directly Imaged by Atomic Force Microscopy. *Nat. Commun.* **2011**, *2*, 449.
- (15) Walter, H.-K.; Bauer, J.; Steinmeyer, J.; Kuzuya, A.; Niemeyer, C. M.; Wagenknecht, H.-A. DNA Origami Traffic Lights” with a Split Aptamer Sensor for a Bicolor Fluorescence Readout. *Nano Lett.* **2017**, *17*, 2467–2472.
- (16) Selnhin, D.; Sparvath, S. M.; Preus, S.; Birkedal, V.; Andersen, E. S. Multifluorophore DNA Origami Beacon as a Biosensing Platform. *ACS Nano* **2018**, *12*, 5699–5708.
- (17) Funck, T.; Nicoli, F.; Kuzyk, A.; Liedl, T. Sensing Picomolar Concentrations of RNA Using Switchable Plasmonic Chirality. *Angew. Chem., Int. Ed.* **2018**, *57*, 13495–13498.
- (18) Douglas, S. M.; Bachelet, I.; Church, G. M. A Logic-Gated Nanorobot for Targeted Transport of Molecular Payloads. *Science* **2012**, *335*, 831–834.
- (19) Anker, J. N.; Hall, W. P.; Lyandres, O.; Shah, N. C.; Zhao, J.; Van Duyne, R. P. Biosensing with Plasmonic Nanosensors. *Nat. Mater.* **2008**, *7*, 442–453.
- (20) Tang, L.; Li, J. Plasmon-Based Colorimetric Nanosensors for Ultrasensitive Molecular Diagnostics. *ACS Sens* **2017**, *2*, 857–875.
- (21) Wu, X.; Hao, C.; Kumar, J.; Kuang, H.; Kotov, N. A.; Liz-Marzán, L. M.; Xu, C. Environmentally Responsive Plasmonic Nanoassemblies for Biosensing. *Chem. Soc. Rev.* **2018**, *47*, 4677–4696.
- (22) Zhou, C.; Duan, X.; Liu, N. DNA-Nanotechnology-Enabled Chiral Plasmonics: From Static to Dynamic. *Acc. Chem. Res.* **2017**, *50*, 2906–2914.
- (23) Hentschel, M.; Schäferling, M.; Duan, X.; Giessen, H.; Liu, N. Chiral Plasmonics. *Sci. Adv.* **2017**, *3*, e1602735.
- (24) Jeong, H.-H.; Mark, A. G.; Lee, T.-C.; Alarcón-Correa, M.; Eslami, S.; Qiu, T.; Gibbs, J. G.; Fischer, P. Active Nanorheology with Plasmonics. *Nano Lett.* **2016**, *16*, 4887–4894.
- (25) Cho, E. J.; Lee, J.-W.; Ellington, A. D. Applications of Aptamers as Sensors. *Annu. Rev. Anal. Chem.* **2009**, *2*, 241–264.

(26) Kuzyk, A.; Schreiber, R.; Zhang, H.; Govorov, A. O.; Liedl, T.; Liu, N. Reconfigurable 3D Plasmonic Metamolecules. *Nat. Mater.* **2014**, *13*, 862–866.

(27) Kuzyk, A.; Yang, Y.; Duan, X.; Stoll, S.; Govorov, A. O.; Sugiyama, H.; Endo, M.; Liu, N. A Light-Driven Three-Dimensional Plasmonic Nanosystem That Translates Molecular Motion into Reversible Chiroptical Function. *Nat. Commun.* **2016**, *7*, 10591.

(28) Kuzyk, A.; Urban, M. J.; Idili, A.; Ricci, F.; Liu, N. Selective Control of Reconfigurable Chiral Plasmonic Metamolecules. *Sci. Adv.* **2017**, *3*, e1602803.

(29) Huizenga, D. E.; Szostak, J. W. A DNA Aptamer That Binds Adenosine and ATP. *Biochemistry* **1995**, *34*, 656–665.

(30) Stojanovic, M. N.; de Prada, P.; Landry, D. W. Fluorescent Sensors Based on Aptamer Self-Assembly. *J. Am. Chem. Soc.* **2000**, *122*, 11547–11548.